Published in final edited form as:
Dev Cell. 2012 March 13; 22(3): 489–500. doi:10.1016/j.devcel.2012.02.005.

ALK1 Signaling Inhibits Angiogenesis by Cooperating with the Notch Pathway

Bruno Larrivée[1], **Claudia Prahst**[1], **Emma Gordon**[1], **Raquel del Toro**[2], **Thomas Mathivet**[2], **Antonio Duarte**[3], **Michael Simons**[1,4], and **Anne Eichmann**[1,2,*]

[1]Yale Cardiovascular Research Center, Section of Cardiovascular Medicine, Department of Internal Medicine, Yale University School of Medicine, New Haven, CT 06511-6664, USA

[2]CIRB Collège de France, Inserm U1050/CNRS UMR7241, 11 Place Marcelin Berthelot, 75005 Paris, France

[3]Centro Interdisciplinar de Investigaçao em Sanidade Animal, Faculdade de Medicina Veterinaria, Technical University of Lisbon, 1300-477 Lisbon, Portugal

[4]Department of Cell Biology, Yale University School of Medicine, New Haven, CT 06520-8002, USA

SUMMARY

Activin receptor-like kinase 1 (ALK1) is an endothelial-specific member of the TGF-β/BMP receptor family that is inactivated in patients with hereditary hemorrhagic telangiectasia (HHT). How ALK1 signaling regulates angiogenesis remains incompletely understood. Here we show that ALK1 inhibits angiogenesis by cooperating with the Notch pathway. Blocking Alk1 signaling during postnatal development in mice leads to retinal hypervascularization and the appearance of arteriovenous malformations (AVMs). Combined blockade of Alk1 and Notch signaling further exacerbates hypervascularization, whereas activation of Alk1 by its high-affinity ligand BMP9 rescues hypersprouting induced by Notch inhibition. Mechanistically, ALK1-dependent SMAD signaling synergizes with activated Notch in stalk cells to induce expression of the Notch targets HEY1 and HEY2, thereby repressing VEGF signaling, tip cell formation, and endothelial sprouting. Taken together, these results uncover a direct link between ALK1 and Notch signaling during vascular morpho-genesis that may be relevant to the pathogenesis of HHT vascular lesions.

INTRODUCTION

Blood vessels form complex branched networks composed of arteries, capillaries, and veins that supply oxygen and nutrients to all body tissues. The luminal side of blood vessels is lined with endothelial cells (ECs), which form an interface between circulating blood in the lumen and the vessel wall and normally rest in a quiescent state. Lack of tissue oxygen and

*Correspondence: anne.eichmann@yale.edu.

SUPPLEMENTAL INFORMATION

Supplemental Information includes four figures and Supplemental Experimental Procedures and can be found with this article online at doi:10.1016/j.devcel.2012.02.005.

nutrient supply triggers EC activation and sprouting of new vessel branches from the preexisting vessel network, a process termed angiogenesis (Geudens and Gerhardt, 2011; Herbert and Stain-ier, 2011). Angiogenesis is initiated by release of growth factors from tissue, and requires coordination of a series of cellular processes including selection of a migrating tip cell at the end of the sprout, and of other ECs, termed stalk cells, which proliferate and form tubes (Wacker and Gerhardt, 2011). A key molecule for the initiation and direction of sprouting is vascular endothelial growth factor A (VEGF-A, hereafter referred to as VEGF). When blood vessels are exposed to VEGF, a number of ECs switch to the tip cell state, whereas others will form the stalk of the vascular sprout (Gerhardt et al., 2003; Larrivée et al., 2009). Tip cells express higher levels of specific molecular markers compared to stalk cells, including platelet-derived growth factor B, VEGF receptor (VEGFR)-2, uncoordinated (UNC)5B, Delta-like (DLL)4, and VEGFR3 (del Toro et al., 2010; Tammela et al., 2008), which are required for proper patterning of the vascular network. The Notch pathway, a key regulator of cell fate, has been shown to be critical to mediate the tip cell/stalk cell switch. VEGF stimulation of tip cells induces high expression of Dll4, a transmembrane Notch ligand, whereas stalk cells preferentially express Jagged1 (Jag1), another Notch ligand (Benedito et al., 2009). Dll4 expression in tip cells induces Notch activation in neighboring stalk cells, which in turn regulate expression of specific target genes including bHLH genes of the Hes/Hey family, and lead to the upregulation of the decoy receptor VEGFR1 and downregulation of VEGFR2 and VEGFR3, therefore limiting the response of these cells to VEGF (Hellström et al., 2007; Lobov et al., 2007; Suchting et al., 2007; Tammela et al., 2008). Newly established lumenized sprouts then remodel into networks supporting blood flow, become specified as arteries or veins, and recruit mural cells to stabilize their walls (Potente et al., 2011). Perfusion of the newly formed networks relieves tissue demand for oxygen and nutrient supply and arrests vessel growth. Major questions in vascular biology are how sprouting ECs coordinate their individual behaviors, and how they build networks with tissue-specific patterning and functionality.

Abnormally patterned blood vessels are seen in many diseases, including hereditary hemorrhagic telangiectasia (HHT) (Dupuis-Girod et al., 2010; Shovlin, 1997). HHT vascular lesions are characterized by direct arteriovenous connections without an intervening capillary bed (Shovlin, 1997, 2010). This results in the formation of telangiectasias and of larger arteriovenous malformations (AVMs), which can be encountered in the lung, brain, and liver. HHT is inherited as an autosomal-dominant trait and affects about 1 in 5,000 people. The abnormal vascular structures in HHT type 1 result from inactivating mutations in *ENG*, which encodes a TGF-β receptor endoglin, whereas those seen in HHT type 2 are caused by mutations in *ACVRL1*, which encodes activin receptor-like kinase 1 (ALK1) (Dupuis-Girod et al., 2010; Johnson et al., 1996). Mutations in *SMAD4* are seen in patients with the combined syndrome of juvenile polyposis and HHT (Gallione et al., 2010). Although it is known that these three mutations disrupt BMP/TGF-b signaling, the exact mechanisms by which they cause the HHT phenotype remain unclear.

ALK1 is an EC-restricted TGF-β type I receptor, which binds to bone morphogenetic protein (BMP) 9, BMP10, and TGF-β. ALK1 leads to the phosphorylation of SMAD1,5,8, which

form active complexes with the common mediator (co) SMAD SMAD4, which then accumulate in the nucleus and act as transcription factors to regulate target gene expression (Orlova et al., 2011). In addition, ALK1 has also been reported to activate extracellular-regulated kinase (ERK) and Jun N-terminal kinase (JNK) pathways (David et al., 2007b).

Genetic, pharmacological, and histopathological evidence points to a critical role for ALK1 signaling in regulating both developmental and pathologic blood vessel formation (Cunha and Pietras, 2011). In murine models, Alk1 deficiency results in early embryonic lethality at E11.5 as a result of defects in the remodeling of the primary capillary plexus into a functional network of arteries, capillaries, and veins (Urness et al., 2000). The ALK1 receptor has long been considered an orphan receptor because it only weakly binds TGF-β. However, recent studies demonstrated that ALK1 could bind BMP9 and the closely related BMP10 (David et al., 2007a; Scharpfenecker et al., 2007). BMP9 is a circulating factor produced mainly by the liver (Bidart et al., 2012), and is present in human serum at around 5 ng/ml (David et al., 2008). BMP9 has been shown to bind with high affinity to both ALK1 and endoglin, as well as to the BMP type II receptor (BMPR-II) and activin type II receptor (ActR-II) (David et al., 2007a; Scharpfenecker et al., 2007). BMP9 inhibits VEGF and FGF-induced migration and proliferation (David et al., 2007a; Scharpfenecker et al., 2007) and has therefore been described as a vascular quiescence factor.

Although recent data have helped understand some of the cellular processes mediated by ALK1, the mechanisms by which ALK1 signaling regulates vascular morphogenesis remain unclear. In zebrafish, the *acvrl1* mutant violet beauregarde presents with vascular malformations with blood flow constrained to a limited number of hyperproliferative cranial vessels, consistent with a role for ALK1 in promoting vascular quiescence during development (Corti et al., 2011; Roman et al., 2002). Alk1 also contributes to homeostasis in mature vessels because global deletion of the *Acvrl1* gene by tamoxifen treatment in postnatal mice results in AVM formation, severe internal hemorrhaging, and lethality (Park et al., 2008, 2009). In addition to BMP/ SMAD signaling, dysregulation of other pathways in arteriovenous specification, including Notch, has been implicated in the formation of AVMs. Interestingly, both gain and loss of Notch signaling can lead to AVM formation (Gale et al., 2004; Krebs et al., 2004, 2010; Murphy et al., 2009, 2012). AVM formation is thought to be due at least in part to defective arteriovenous specification, but the mechanisms by which Notch and ALK1 signaling mediate this process remain largely unknown.

Here we describe a cooperation between the Notch and ALK1 signaling pathways during tip/stalk specification in sprouting angiogenesis. We demonstrate that decreased ALK1 signaling results in EC hypersprouting, and that this effect is caused, at least in part, by reduced SMAD-induced HEY1 and HEY2 expression. Furthermore, we show that both ALK1 and Notch signaling can partially compensate for each other in loss-of-function studies.

RESULTS

Blocking Alk1 Induces Hypervascularization and AVM Formation

We investigated Alk1 expression and the effects of Alk1 inhibition on blood vessel development in postnatal mice using the retinal angiogenesis model. Whole-mount staining of P7 retinas with an anti-Alk1 antibody showed strong Alk1 expression in arteries, and lower receptor levels in veins and the capillary plexus (see Figure S1A available online), as previously reported in *Alk1-lacZ* reporter mice (Seki et al., 2003). At the leading edge of the retina, Alk1 expression was stronger in stalk cells than in tip cells (Figure S1A). ELISA measurement of circulating serum Bmp9 levels at different stages of postnatal development revealed high levels in P6 mice (~1.5 ng/ml) that progressively decreased to stabilize at 8 weeks at ~100 pg/ml (Figure S1B). These data suggested that circulating Bmp9 might activate Alk1 on lumenized postnatal retinal vessels, including stalk cells.

To examine effects of ALK1 blockade, we generated an adenovirus encoding the ALK1 extracellular domain (amino acids 1–118 of human ALK1) fused to the Fc portion of human immunoglobulin (ALK1Fc), which acts as a ligand trap and blocks ALK1 signaling in vivo (Niessen et al., 2010). Intraperito-neal injection of the ALK1Fc virus into neonatal P1 mice induces complete disappearance of circulating serum Bmp9 (Figure S1C). ALK1Fc-treated mice developed striking retinal hyper-vascularization already 3 days after virus injection at P4 (Figures 1A and 1B). At P6, ALK1Fc-treated mice developed a dense sheet of vessels, with a significant increase in vascularized area compared to control virus-injected mice (Figures 1C and 1D). At P12, ALK1Fc-treated mice showed defective vessel remodeling and arterial patterning defects (Figures 1E–1L). Control virus-injected retinas had five to six thin, straight arteries radiating out from the optic nerve that were connected to a regular network of capillaries and veins (Figures 1E–1H). In contrast, ALK1Fc-treated mice showed fewer and dilated, tortuous arteries developing in a hyperbranched, dense capillary plexus (Figures 1I–1L). Remodeling of vessels of the ear, which are actively growing during the treatment period, was also affected in ALK1Fc-treated mice, and AVMs had developed in ears of all treated mice at P12 (Figure 1M).

Adenoviral overexpression of Bmp9 during the first postnatal week proved difficult, and we failed to obtain consistently elevated serum levels of Bmp9 beyond the already high endogenous expression levels at P6 (Figure S1B). At P12, serum levels of Adeno-Bmp9-treated mice were consistently higher than those of control mice and led to significantly decreased neovascularization of the deeper retinal vessel layer (Figures 1N–1P and S1D). Taken together, these data show that Bmp9 can inhibit retinal angiogenesis, whereas blocking Bmp9-Alk1 signaling induces retinal hypervascularization, an effect that is similar to that observed after inhibition of the Notch signaling pathway.

BMP9/ALK1 Modulates Endothelial Notch Response In Vitro and In Vivo

To test how BMP9/ALK1 signaling affects sprouting angiogenesis, we cultured human umbilical vein endothelial cells (HUVECs) in 3D fibrin gels and induced tube formation with VEGF (Figures 2A and 2B). Recombinant BMP9 protein efficiently suppressed VEGF-induced tube formation (Figures 2A and 2B), which may be due in part to antiproliferative

effects (Figure S2A) (David et al., 2007a, 2008; Scharpfenecker et al., 2007). Blocking of BMP9/ALK1 signaling using ALK1Fc virus-infected cells enhanced VEGF-induced tube formation (Figures 2A and 2B). It is noteworthy that ALK1 inhibition had limited effect on endothelial sprouting in the absence of VEGF in vitro (Figures S2B and S2C), suggesting that ALK1 blockade may promote angiogenesis only in the presence of proangiogenic stimuli. This was confirmed in vivo by the observation that ALK1 inhibition did not affect mature established vessels in the skin (Figure S2D).

To test if ALK1 signaling intersects with the Notch pathway, we blocked both ALK1 and Notch using ALK1Fc and DAPT. Combined blockade of both pathways further enhanced tube formation compared to blockade of each pathway alone (Figures 2A and 2B), indicating that ALK1 and Notch signaling pathways may interact to inhibit VEGF-induced sprouting. We next examined the effects of activating one pathway while blocking the other. Jagged-1 (JAG1) peptide-mediated activation of the Notch pathway was able to suppress ALK1Fc-mediated hypersprouting, whereas a control-scrambled peptide that does not activate Notch did not affect sprouting (Figures 2A and 2B; data not shown). Likewise, BMP9 was able to reverse the hypersprouting induced by DAPT (Figures 2A and 2B).

Our in vitro data predicted that combined Alk1 and Notch inhibition in vivo should exacerbate hypervascularization. We tested this hypothesis by injecting an anti-Bmp9 blocking antibody into *Dll4*$^{+-}$ pups, which show increased tip cell specification and hypersprouting (Suchting et al., 2007). Blockade of Bmp9 induced retinal hyper-vascularization (Figures 2C and 2D), confirming that the effects of ALK1Fc (Figures 1A–1D) are likely due to decreased circulating Bmp9 levels. *Dll4*$^{+/-}$ mice showed significant hypervascularization when compared to wild-type littermates (Figures 2C and 2D). Combined blockade of Alk1 and Notch signaling further increased hypervascularization when compared to *Dll4*$^{+/-}$ or anti-Bmp9-treated wild-type mice (Figures 2C and 2D).

Our in vitro data further predicted that activation of Alk1 signaling should rescue defects induced by Notch inhibition. To confirm this experimentally, we used DAPT-treated mice, which received intraocular injections of PBS in one eye and BMP9 in the other. Twelve hours afterward, DAPT-induced Notch blockade resulted in increased tip cell formation, determined by quantification of filopodia-extending cells in the vascular front of the retina (Figures 2E and 2F). BMP9 injection induced a dramatic decrease in the number of filopodia-extending cells in control- and DAPT-treated mice (Figures 2E and 2F). Taken together, the results indicate that BMP9 signaling counteracted hypersprouting induced by Notch inhibition in vitro and in vivo.

BMP9/ALK1 Signaling Induces Notch Target Gene Expression

We next examined signaling events induced by ALK1 activation to determine if ALK1 and Notch converge on common downstream pathways. BMP9 stimulation of HUVECs induced rapid phosphorylation of SMAD1,5,8 as well as phosphorylation of ERK1,2 (Figure 3A). BMP9 also induced expression of the inhibitory SMAD6 2 hr after growth factor addition (Figure 3A). SMAD1,5,8 and ERK activation was ALK1 dependent, as shown by siRNA-mediated knockdown of *ALK1*, which abolished BMP9-mediated SMAD phosphorylation and decreased phospho-ERK levels (Figure 3B). To examine downstream target genes

induced by Notch and ALK1 activation, we seeded HUVECs onto plates coated with recombinant sDll4 protein to activate Notch signaling alone or in the presence of BMP9. BMP9 but not Dll4 induced expression of ALK1 targets *ID1* and transcription of *SMAD6* and *SMAD7* (Figure 3C). Dll4 induced expression of Notch target genes *HES1* (data not shown), *HEY1*, and *HEY2* and upregulated *JAG1* levels (Figure 3D). Dll4 did not affect *ALK1* mRNA levels (data not shown). Strikingly, BMP9 treatment alone also induced expression of *HES1* (data not shown), *HEY1*, *HEY2*, and *JAG1* (Figure 3D). mRNA expression by BMP9 was induced within 1 hr, and was independent of protein synthesis (Figure S3A), indicating that BMP9 signaling directly controls expression of these genes, which is consistent with a recent study showing direct binding of SMAD1,5 to the HEY1, HEY2, and JAG1 promoters (Morikawa et al., 2011). Combined ALK1 and Notch activation synergized to activate expression of *HEY1* and *HEY2*, with *HEY2* levels increasing more than 1,000-fold after 24 hr treatment (Figure 3D). BMP9 and Dll4 also additively induced expression of the vascular guidance receptor *UNC5B*, and of *VEGFR1*, which both counteract VEGF signaling (Herbert and Stainier, 2011; Koch et al., 2011), and inhibited expression of the tip cell marker *apelin* (Figure 3E) (del Toro et al., 2010).

Analysis of Jag1 and VEGFR1 expression in retinal vessels following intraocular BMP9 injections showed that both proteins were upregulated in the angiogenic front of BMP9-treated compared to control PBS-injected eyes (Figures S3B and S3C), indicating that the gene expression changes observed in vitro following BMP9 activation of ALK1 signaling were also seen in vivo. Taken together, these data show that BMP9-ALK1 cooperates with the Notch signaling pathway to activate downstream gene expression, including activation of Notch targets, inhibitors of VEGF signaling, and suppression of tip cell markers.

BMP9 Suppression of Angiogenesis Requires SMAD4, HEY1, and HEY2

We next asked how BMP9-ALK1 downstream signaling could mechanistically affect Notch signaling. Because BMP9-mediated ALK1 activation leads to SMAD1,5,8 phosphorylation and ERK activation (Figure 2A), we tested if activation of ERK and/ or SMAD was required for BMP9-ALK1-mediated sprouting inhibition and induction of Notch target genes. ERK inhibition using the pharmacological inhibitor U0126 did not affect BMP9-mediated induction of Notch targets *HEY1* and *HEY2* (Figures S4A and S4B). ERK inhibition also did not change BMP9-mediated inhibition of VEGF-induced HUVEC tube formation in 3D cultures (Figures S4C and S4D), indicating that this pathway is dispensable for ALK1 effects on sprouting and gene expression.

In contrast, siRNA-mediated knockdown of *SMAD4* (Figure S4E), which prevents the formation of the active SMAD complex, suppressed BMP9-mediated inhibition of HUVEC sprouting and abolished BMP9-mediated induction of *ID1*, *HEY1*, *HEY2*, and *JAG1* (Figures 4A–4C and 4G). Taken together, these data show that SMAD signaling is required for BMP9-ALK1 downstream activation of target gene expression and sprouting inhibition.

Because SMAD signaling was required for induction of Notch target gene expression, we reasoned that HEY1 and HEY2 might be required for BMP9-mediated inhibition of HUVEC sprouting. siRNA-mediated knockdown of *HEY1* and *HEY2* (Figure S4E) suppressed BMP9-mediated inhibition of tube formation and effects on downstream gene expression

(Figures 4A, 4D, 4E, and 4G). In contrast, knockdown of RBPJ did not affect BMP9-mediated suppression of tube formation or induction of *HEY1* and *HEY2* (Figures 4F, 4G, and S4E), supporting a model whereby BMP9-ALK1-induced SMAD signaling induces HEY1 and HEY2 independently of canonical Notch activation.

Alk1 Signaling Inhibits Tip Cell Selection

Because both ALK1 and Notch are expressed preferentially in stalk cells, and inhibit sprouting in vivo and in vitro, we next asked whether ALK1 signaling could affect endothelial tip/stalk cell specification. Using mosaic bead-sprouting assays in which target-specific siRNA-transfected cells were mixed with control siRNA transfected cells, we found that *ALK1* knockdown ECs were more likely to be present at the tip position of endothelial sprouts compared to control siRNA (Figures 5A–5C). Furthermore, inhibition of SMAD signaling using *SMAD4* siRNA or knockdown of *HEY2* also resulted in increased frequency of ECs at the tip position (Figures 5C–5E). Taken together, these results support a model in which ALK1 signaling in stalk cells, through SMAD1,5,8 and downstream expression of ALK1 targets including HEY transcription factors, prevents tip cell specification and migration and participates in keeping ECs in the stalk cell state (Figure 6).

DISCUSSION

The data presented here demonstrate an antiangiogenic role of ALK1 during early postnatal angiogenesis because inhibition of this receptor with an ALK1Fc ligand trap resulted in excessive sprouting angiogenesis. Hypervascularization in ALK1Fc-treated mice was followed by arteriovenous mispatterning and AVM formation. Likewise, hypervascularization was found to precede appearance of HHT vascular lesions in other animal models of HHT, including *Acvrl1* and *ENG*-inducible mouse knockouts and zebrafish *acvrl1* mutants (Corti et al., 2011; Lebrin et al., 2010; Mahmoud et al., 2010; Park et al., 2009; Roman et al., 2002). Together, these data suggest that excessive rather than insufficient angiogenesis may be a contributing factor to HHT lesion formation. Furthermore, ALK1 has been reported to play a role in transducing hemodynamic forces (Corti et al., 2011), and altered blood flow in the absence of ALK1 signaling may participate in the formation of HHT lesions. The effect of ALK1 blockade on angiogenesis was VEGF dependent, cautioning against the use of ALK1 inhibitors to treat pathological tumor angiogenesis (Hu-Lowe et al., 2011; Mitchell et al., 2010) because it indicates that ALK1 inhibition may lead to appearance of vascular lesions in regions of active angiogenesis.

The hypervascularization observed in the retina of ALK1Fc-injected pups presented striking similarities to that observed in mice with genetic deletion of *Dll4* or other Notch signaling components (Hellström et al., 2007; Lobov et al., 2007; Suchting et al., 2007). This led us to ask whether the Notch and ALK1 pathways interacted to regulate sprouting angiogenesis. Surprisingly, we observed that SMAD signaling downstream of BMP9-ALK1 activated transcription of canonical Notch targets *HES1*, *HEY1*, and *HEY2*, as well as the Notch ligand *JAG1*, and synergized with activated Notch in inducing expression of some of these genes. Furthermore, we showed that SMAD4, HEY1, and HEY2 are required for BMP9-mediated inhibition of sprouting and induction of downstream gene expression. SMAD-mediated

induction of Notch targets did not appear to require canonical Notch signaling because knockdown of RBPJ did not affect BMP9-mediated sprouting inhibition or *HEY1* and *HEY2* induction (Figures 4F and 4G). A recent study has reported direct binding of SMAD1,5 to the HEY1, HEY2, JAG1, and UNC5B promoter following EC activation by BMP9 (Morikawa et al., 2011), supporting a model whereby BMP9-ALK1-induced SMAD signaling induces transcription of select Notch target genes independently of canonical Notch activation, and synergizes with activated Notch-RBPJ to fully induce transcription of these targets (Figure 6). Alternatively, previous studies have shown a direct interaction between activated SMADS and the Notch intracellular domain, which can stimulate SMAD binding to DNA and produce a functional synergy following BMP stimulation of ECs (Dahlqvist et al., 2003; Itoh et al., 2004; Li et al., 2011). In addition, Notch has been reported to regulate SMAD1, SMAD2, and SMAD3 expression levels, thereby modulating TGF-β signaling in ECs (Fu et al., 2009). The precise molecular mechanisms of interaction between the SMAD and Notch signaling pathway in ECs following ALK1 activation remain to be established.

HEY1 and HEY2 are well-established Notch targets in vascular development (Zhong et al., 2000). Mouse embryos lacking both *Hey1* and *Hey2* are embryonic lethal due to severe cardiovascular malformations highly similar to those seen after inactivation of Notch signaling components (Fischer et al., 2004). HEY1 has been shown to inhibit VEGFR2 expression downstream of Notch by direct binding to the VEGFR2 promoter (Taylor et al., 2002), thereby decreasing VEGF response. In line with these findings, we found that VEGFR2 levels increased significantly following *HEY2* siRNA-mediated knockdown in a SMAD-independent manner (data not shown), indicating that decreased VEGFR2 expression by synergistic induction of *HEY2* following ALK1 and Notch activation may contribute to inhibiting VEGF response in stalk cells. Likewise, BMP9-ALK1 signaling increases VEGFR1 levels, thereby inhibiting VEGF response in stalk cells. Furthermore, BMP9-ALK1 induces JAG1 expression, which contributes to tip-stalk cell selection by antagonizing Dll4 expression in tip cells (Benedito et al., 2009). We also observed that UNC5B was a direct target of ALK1 signaling. UNC5B is expressed in tip and stalk cells and arterial endothelium, but not in veins (Larrivée et al., 2007; Lu et al., 2004). UNC5B expression is induced by VEGF and the homeobox transcription factor HLX in tip cells (Testori et al., 2011), and appears to be regulated by ALK1 in stalk cells and arteries. UNC5B counteracts VEGF signaling, as shown by function-blocking approaches (Koch et al., 2011), which may contribute to tip-stalk cell selection and/or arterial integrity and vessel quiescence. Finally, we show that Notch signaling and ALK signaling cooperate to decrease expression of the tip cell marker apelin, a secreted polypeptide that induces stalk cell proliferation via its receptor APLNR (del Toro et al., 2010; Kasai et al., 2008). Together with the mosaic experiments, which show that ALK1, SMAD, and HEY-deficient cells more frequently occupy the tip position of growing vessel sprouts, these data suggest that ALK1 signaling and Notch signaling cooperate in stalk cells to inhibit conversion into tip cells.

Our results show that in addition to activation by Dll4, circulating factors such as BMP9 reinforce Notch signaling by binding to cognate receptors on stalk cells, together coordinating stalk to tip cell conversion and angiogenic sprouting. Notch activation is also

positively modulated by inputs from the basement membrane (Estrach et al., 2011; Stenzel et al., 2011). Sprouting ECs express integrin receptors and deposit basement membrane components, including nidogens and laminins for stalk cells to migrate on (del Toro et al., 2010; Germain et al., 2010). Laminin-mediated integrin signaling promotes Dll4 expression, thereby reinforcing Notch signaling in stalk cells and maintaining the stalk cell state (Estrach et al., 2011; Stenzel et al., 2011). Therefore, Notch signaling in stalk cells is regulated by inputs from neighboring cells, the basement membrane, and the circulation.

Our data show that BMP9 through ALK1 functions to limit tip cell formation. During angiogenic sprouting, an individual tip cell is estimated to occupy the lead position of a capillary sprout for only a limited period of time (approximately 4 hr), after which it is overtaken by another cell (Jakobsson et al., 2010). This “team effort” of tip and stalk cells to ensure capillary guidance is coor dinated by dynamic interplay between VEGF and Notch signaling (Geudens and Gerhardt, 2011; Herbert and Stainier, 2011; Potente et al., 2011). Our data suggest that ALK1 signaling contributes to this oscillatory behavior in vivo. BMP9 circulates in the bloodstream during early postnatal development at levels well above its reported EC_{50} in human micro-vascular endothelium (EC_{50} = 45 ± 27 pg/ml) (David et al., 2007a). Although the EC_{50} of Bmp9 on mouse endothelium in vivo is not known, we expect that the Bmp9 levels are sufficient to fully activate Alk1 in retinal vessels. BMP10 may also modulate retinal angiogenesis. In addition to stalk cells and arterial ECs, which express highest levels of ALK1, tip cells may also be exposed to extravasated tissue BMP9, given that immature, developing vessels are leaky. The high levels of circulating BMP9 and the robust effects of ALK1 signaling on stalk cell gene expression are somewhat at odds with active stalk to tip cell conversion, suggesting that BMP9 signaling may be decreased in tip cells, perhaps by inhibitory SMAD6 and SMAD7. In addition, it is possible that BMP antagonists may modulate BMP9 activity in the vasculature, even though BMP9 and BMP10 have not been reported to interact with BMP antagonists noggin or follistatin (Harrington et al., 2006; Seemann et al., 2009).

BMPs have been described both as pro- and antiangiogenic factors depending on the cellular context (David et al., 2008; Suzuki et al., 2010). BMP signaling strongly induces expression of *ID1*, which promotes endothelial proliferation and migration (Valdimarsdottir et al., 2002). BMP9 also robustly induced *ID1* expression but suppressed EC sprouting. ALK1 induced expression of *HEY1* and *HEY2*, which have been shown to antagonize ID1 (Itoh et al., 2004), and would therefore suppress its stimula-tory effects on angiogenesis. The relative levels of induction of *ID1* and *HEY* transcription factors by different BMPs may potentially contribute to the different activities of BMPs on angiogenesis, with antiangiogenic BMPs (BMP9, BMP10) inducing high levels of HEY and therefore lower levels of ID1 activity. Activation of ID1 by BMP9 underscores that BMP9-ALK1 signaling also influences angiogenic sprouting by mechanisms that are independent of Notch signaling.

The results shown here suggest that altered Notch signaling may contribute to AVMs in patients with HHT type 2 with *ACVRL1* mutations. Both Notch loss- and gain-of function mutations cause AVMs (Gale et al., 2004; Krebs et al., 2004, 2010; Murphy et al., 2009, 2012), but interestingly, the phenotype of the *Acvrl1* knockout mice is more reminiscent of

Notch gain-of-function mutants (Park et al., 2009). In addition, inducible overexpression of active Notch in transgenic mice has been shown to induce AVMs, which were resolved following arrest of transgene expression (Miniati et al., 2010). Furthermore, human brain AVMs showed increased Notch and Notch ligand expression, suggesting that once AVMs are established, they exhibit increased Notch activation. Whether decreased Notch activation and subsequent hypervascularization following ALK1 blockade contribute to the initial steps of AVM formation in human HHT lesions remains to be investigated.

EXPERIMENTAL PROCEDURES

Additional methods can be found in Supplemental Experimental Procedures.

Antibodies and Recombinant Proteins

Antibodies against Jag1 (AF599), Bmp9 (AF3209), VEGFR1 (AF471), and Alk1 (AF770) were purchased from R&D Systems (Minneapolis, MN, USA), anti-CD31 (clone MEC 13.3) was obtained from BD Biosciences, and anti-smooth muscle actin (SMA) (clone 1A4) was obtained from Sigma-Aldrich. IsolectinB4 and secondary antibodies were purchased from Molecular Probes (Invitrogen). For western blot analysis, antibodies against P-SMAD1,5,8 (9511), SMAD1 (9743), SMAD6 (9519), P-ERK1/2 (4370), and ERK1/2 (4695) were acquired from Cell Signaling Technology (Beverly, MA, USA). Calcein AM was purchased from Invitrogen. Recombinant sDll4, BMP9, and VEGF-A were obtained from R&D Systems. DAPT was purchased from Calbiochem. The 17-mer JAG1 peptide (CDDYYYGFGCNKFCRPR), corresponding to amino acids 187–203 of human JAG1, was previously described (Hellström et al., 2007). The scrambled peptide (SC)-JAG1 (RCGPDCFDNYGRYKYCF) was used as a negative control. Both peptides were synthesized by the Yale W.M. Keck Foundation. Peptides were dissolved in DMSO (50 mM), aliquoted, and stored at —20°C. Adenoviral constructs are described in Supplemental Experimental Procedures.

Mice

C57/Bl6 mice (Jackson Laboratories) were maintained in the Animal Research Center at Yale University. All experiments were approved by the IACUC of Yale University. The *Dll4*$^{+-}$ (CD1) mice have been previously described (Suchting et al., 2007). To inhibit the Notch pathway, the g-secretase inhibitor DAPT (Calbiochem), dissolved in sterile sunflower oil, was subcutaneously injected twice into mice (100 mg/kg) at P4, and the mice were sacrificed 24 hr following injection. Injection with sunflower oil was used as a negative control. Anti-Bmp9 (10 mg/kg) was injected intraperitoneally at P1 and P3. Latex blue injections were performed as previously described (Park et al., 2009).

Intraocular BMP9 Injections

A total of 1 μl of 0.5 mg/ml BMP9 dissolved in PBS or 1 ml PBS was injected into the eyes of anesthetized P4 mice with a PicoSpritzer III (Intracel, Herts, UK). Mice were sacrificed 16 hr later, and the retinas were isolated for immunohistochemistry and IsolectinB4 staining.

Cell Culture

HUVECs were obtained from Lonza and cultured in ECGM-2 (Lonza). HEK293 cells were cultured in DMEM (Invitrogen) supplemented with 10% FCS and penicillin/streptomycin at 37°C in 5% CO_2. HUVECs were starved overnight in EBM-2 supplemented with 0.1% FBS prior to stimulation with 10 ng/ml BMP9 and/or 25 ng/ml VEGF. To assess the effect of BMP9 on gene expres sion in the absence of protein synthesis, HUVECs were treated with BMP9 in the presence of 10 μml cycloheximide (Sigma-Aldrich). For stimulation with sDll4, 6-well plates were precoated with 10 mg/ml sDll4 before plating cells. DAPT was dissolved as a 1 mM solution in DMSO and was used at a final concentration of 2 μM. JAG1 peptide was used at 1 μM.

siRNA Transfection

siRNAs (FlexiTube siRNA) were purchased from QIAGEN. HUVECs were transfected with 25 pmol siRNA per 6-well with 2.5 μl RNAiMax (Invitrogen) according to the instructions of the manufacturer. Cells were used for experiments 48 hr after transfection.

Sprouting Assay

After siRNA transfection, HUVECs (250,000 cells/well in 6-well plates) were resuspended in 300 μl fibrinogen solution (2.5 mg/ml fibrinogen [Sigma-Aldrich] in EBM-2 [Lonza] supplemented with 2% FBS and 50 μg/ml aprotinin [Sigma-Aldrich]), and plated on top of a precoated fibrin layer (400 μl fibrinogen solution clotted with 1 U thrombin [Sigma-Aldrich] for 20 min at 37°C). The second layer of fibrin was clotted for 1 hr at 37°C. C3H10T1/2 cells (250,000 cells/well), in EBM-2 supplemented with 2% FBS and 25 ng/ml VEGF, were then plated on top of the fibrin layers. Cultures were incubated at 37°C, 5% CO_2. Control cultures were grown with VEGF for 2–3 days, VEGF was then removed, and cultures were grown for another 2–3 days. Growth factors (VEGF, BMP9), DAPT, JAG1, or ALK1Fc were added after 2–3 days. After 4–6 days, cultures were labeled with 4 μg/ml Calcein AM for 1 hr, and imaged by fluorescence using a standard FITC filter.

For bead-sprouting assays, HUVECs transfected with siRNA 24 hr prior were labeled with either PKH26 (red) or PKH67 (green) dyes (Sigma-Aldrich) according to the instruction of the manufacturer, and coated on cytodex3 microcarrier beads (Sigma-Aldrich) for 24 hr before embedding in a fibrin gel. Sprouts were imaged 2–4 days later.

Immunohistochemistry on Whole-Mount Retinas

In brief, after sacrificing the animals, the eyes were removed and prefixed in 4% PFA for 20 min at room temperature. The dissected retinas were blocked overnight at 4°C in Tris-HCl 0.1 M-NaCl 150 mM-Blocking Reagent (Pierce)

(TNB)-0.5% Triton X-100. Primary antibodies were then incubated with the retinas overnight in TNB/0.5% Triton X-100. After washing, the retinas were incubated with IsolectinB4 in Pblec (1 mM $MgCl_2$, 1 mM $CaCl_2$, 0.1 mM $MnCl_2$, 1% Triton X-100 in PBS) overnight, incubated with the corresponding secondary antibody for 2 hr at room temperature, and mounted in fluorescent mounting medium (DAKO, Carpinteria, CA, USA). Images were acquired on a Nikon eclipse Ti confocal microscope with the

PerkinElmer UltraVIEW Confocal Imaging System and PerkinElmer Volocity software, and a Leica M205 FA microscope with the Leica Application Suite (LAS) software.

Statistical Analyses

A two-tailed, unpaired Student's t test was done to determine statistical significance by calculating the probability of difference between two means (Graph-Pad Prism 4; GraphPad Software, La Jolla, CA, USA). Differences were considered statistically significant for p values of 0.05 or less (*$p < 0.05$, **$p < 0.01$, ***$p < 0.005$). Error estimates are displayed as SEM.

Supplementary Material

Refer to Web version on PubMed Central for supplementary material.

Acknowledgments

We thank Suk-Won Jin for critical reading of the manuscript. This work was supported by grants from Fondation Leducq (Artemis Transatlantic Network of Excellence), Edward N. and Della L. Thome Memorial Foundation, Fondation Bettencourt, Inserm, Agence Nationale de la Recherche, and Fondation pour la Recherche Médicale (FRM). C.P. was supported by Deutsche Forschungsgemeinschaft. E.G. was supported by a Brown-Coxe fellowship. R.d.T. and T.M. were supported by FRM.

REFERENCES

Benedito R, Roca C, Sörensen I, Adams S, Gossler A, Fruttiger M, Adams RH. The notch ligands Dll4 and Jagged1 have opposing effects on angiogenesis. Cell. 2009; 137:1124–1135. [PubMed: 19524514]

Bidart M, Ricard N, Levet S, Samson M, Mallet C, David L, Subileau M, Tillet E, Feige JJ, Bailly S. BMP9 is produced by hepatocytes and circulates mainly in an active mature form complexed to its prodomain. Cell. Mol. Life Sci. 2012; 69:313–324. [PubMed: 21710321]

Corti P, Young S, Chen CY, Patrick MJ, Rochon ER, Pekkan K, Roman BL. Interaction between alk1 and blood flow in the development of arteriovenous malformations. Development. 2011; 138:1573–1582. [PubMed: 21389051]

Cunha SI, Pietras K. ALK1 as an emerging target for antiangiogenic therapy of cancer. Blood. 2011; 117:6999–7006. [PubMed: 21467543]

Dahlqvist C, Blokzijl A, Chapman G, Falk A, Dannaeus K, Ibâñez CF, Lendahl U. Functional Notch signaling is required for BMP4-induced inhibition of myogenic differentiation. Development. 2003; 130:6089–6099. [PubMed: 14597575]

David L, Mallet C, Mazerbourg S, Feige JJ, Bailly S. Identification of BMP9 and BMP10 as functional activators of the orphan activin receptor-like kinase 1 (ALK1) in endothelial cells. Blood. 2007a; 109:1953–1961. [PubMed: 17068149]

David L, Mallet C, Vailhé B, Lamouille S, Feige JJ, Bailly S. Activin receptor-like kinase 1 inhibits human microvascular endothelial cell migration: potential roles for JNK and ERK. J. Cell. Physiol. 2007b; 213:484–489. [PubMed: 17620321]

David L, Mallet C, Keramidas M, Lamandé N, Gasc JM, Dupuis-Girod S, Plauchu H, Feige JJ, Bailly S. Bone morphogenetic protein-9 is a circulating vascular quiescence factor. Circ. Res. 2008; 102:914–922. [PubMed: 18309101]

del Toro R, Prahst C, Mathivet T, Siegfried G, Kaminker JS, Larrivee B, Breant C, Duarte A, Takakura N, Fukamizu A, et al. Identification and functional analysis of endothelial tip cell-enriched genes. Blood. 2010; 116:4025–4033. [PubMed: 20705756]

Dupuis-Girod S, Bailly S, Plauchu H. Hereditary hemorrhagic telangiectasia: from molecular biology to patient care. J. Thromb. Haemost. 2010; 8:1447–1456. [PubMed: 20345718]

Estrach S, Cailleteau L, Franco CA, Gerhardt H, Stefani C, Lemichez E, Gagnoux-Palacios L, Meneguzzi G, Mettouchi A. Laminin-binding integrins induce Dll4 expression and Notch signaling in endothelial cells. Circ. Res. 2011; 109:172–182. [PubMed: 21474814]

Fischer A, Schumacher N, Maier M, Sendtner M, Gessler M. The Notch target genes Hey1 and Hey2 are required for embryonic vascular development. Genes Dev. 2004; 18:901–911. [PubMed: 15107403]

Fu Y, Chang A, Chang L, Niessen K, Eapen S, Setiadi A, Karsan A. Differential regulation of transforming growth factor beta signaling pathways by Notch in human endothelial cells. J. Biol. Chem. 2009; 284:19452–19462. [PubMed: 19473993]

Gale NW, Dominguez MG, Noguera I, Pan L, Hughes V, Valenzuela DM, Murphy AJ, Adams NC, Lin HC, Holash J, et al. Haploinsufficiency of delta-like 4 ligand results in embryonic lethality due to major defects in arterial and vascular development. Proc. Natl. Acad. Sci. USA. 2004; 101:15949–15954. [PubMed: 15520367]

Gallione C, Aylsworth AS, Beis J, Berk T, Bernhardt B, Clark RD, Clericuzio C, Danesino C, Drautz J, Fahl J, et al. Overlapping spectra of SMAD4 mutations in juvenile polyposis (JP) and JP-HHT syndrome. Am. J. Med. Genet. A. 2010; 152A:333–339. [PubMed: 20101697]

Gerhardt H, Golding M, Fruttiger M, Ruhrberg C, Lundkvist A, Abramsson A, Jeltsch M, Mitchell C, Alitalo K, Shima D, Betsholtz C. VEGF guides angiogenic sprouting utilizing endothelial tip cell filopodia. J. Cell Biol. 2003; 161:1163–1177. [PubMed: 12810700]

Germain S, Monnot C, Muller L, Eichmann A. Hypoxia-driven angiogenesis: role of tip cells and extracellular matrix scaffolding. Curr. Opin. Hematol. 2010; 17:245–251. [PubMed: 20308893]

Geudens I, Gerhardt H. Coordinating cell behaviour during blood vessel formation. Development. 2011; 138:4569–4583. [PubMed: 21965610]

Harrington AE, Morris-Triggs SA, Ruotolo BT, Robinson CV, Ohnuma S, Hyvönen M. Structural basis for the inhibition of activin signalling by follistatin. EMBO J. 2006; 25:1035–1045. [PubMed: 16482217]

Hellström M, Phng LK, Hofmann JJ, Wallgard E, Coultas L, Lindblom P, Alva J, Nilsson AK, Karlsson L, Gaiano N, et al. Dll4 signalling through Notch1 regulates formation of tip cells during angiogenesis. Nature. 2007; 445:776–780. [PubMed: 17259973]

Herbert SP, Stainier DY. Molecular control of endothelial cell behaviour during blood vessel morphogenesis. Nat. Rev. Mol. Cell Biol. 2011; 12:551–564. [PubMed: 21860391]

Hu-Lowe DD, Chen E, Zhang L, Watson KD, Mancuso P, Lappin P, Wickman G, Chen JH, Wang J, Jiang X, et al. Targeting activin receptor-like kinase 1 inhibits angiogenesis and tumorigenesis through a mechanism of action complementary to anti-VEGF therapies. Cancer Res. 2011; 71:1362–1373. [PubMed: 21212415]

Itoh F, Itoh S, Goumans MJ, Valdimarsdottir G, Iso T, Dotto GP, Hamamori Y, Kedes L, Kato M, ten Dijke Pt P. Synergy and antagonism between Notch and BMP receptor signaling pathways in endothelial cells. EMBO J. 2004; 23:541–551. [PubMed: 14739937]

Jakobsson L, Franco CA, Bentley K, Collins RT, Ponsioen B, Aspalter IM, Rosewell I, Busse M, Thurston G, Medvinsky A, et al. Endothelial cells dynamically compete for the tip cell position during angiogenic sprouting. Nat. Cell Biol. 2010; 12:943–953. [PubMed: 20871601]

Johnson DW, Berg JN, Baldwin MA, Gallione CJ, Marondel I, Yoon SJ, Stenzel TT, Speer M, Pericak-Vance MA, Diamond A, et al. Mutations in the activin receptor-like kinase 1 gene in hereditary haemorrhagic telangiectasia type 2. Nat. Genet. 1996; 13:189–195. [PubMed: 8640225]

Kasai A, Shintani N, Kato H, Matsuda S, Gomi F, Haba R, Hashimoto H, Kakuda M, Tano Y, Baba A. Retardation of retinal vascular development in apelin-deficient mice. Arterioscler. Thromb. Vasc. Biol. 2008; 28:1717–1722. [PubMed: 18599802]

Koch AW, Mathivet T, Larrivée B, Tong RK, Kowalski J, Pibouin-Fragner L, Bouvrée K, Stawicki S, Nicholes K, Rathore N, et al. Robo4 maintains vessel integrity and inhibits angiogenesis by interacting with UNC5B. Dev. Cell. 2011; 20:33–46. [PubMed: 21238923]

Krebs LT, Shutter JR, Tanigaki K, Honjo T, Stark KL, Gridley T. Haploinsufficient lethality and formation of arteriovenous malformations in Notch pathway mutants. Genes Dev. 2004; 18:2469–2473. [PubMed: 15466160]

Krebs LT, Starling C, Chervonsky AV, Gridley T. Notch1 activation in mice causes arteriovenous malformations phenocopied by ephrinB2 and EphB4 mutants. Genesis. 2010; 48:146–150. [PubMed: 20101599]

Larrivée B, Freitas C, Trombe M, Lv X, Delafarge B, Yuan L, Bouvrée K, Bréant C, Del Toro R, Bréchot N, et al. Activation of the UNC5B receptor by Netrin-1 inhibits sprouting angiogenesis. Genes Dev. 2007; 21:2433–2447. [PubMed: 17908930]

Larrivée B, Freitas C, Suchting S, Brunet I, Eichmann A. Guidance of vascular development: lessons from the nervous system. Circ. Res. 2009; 104:428–441. [PubMed: 19246687]

Lebrin F, Srun S, Raymond K, Martin S, van den Brink S, Freitas C, Bréant C, Mathivet T, Larrivée B, Thomas JL, et al. Thalidomide stimulates vessel maturation and reduces epistaxis in individuals with hereditary hemorrhagic telangiectasia. Nat. Med. 2010; 16:420–428. [PubMed: 20364125]

Li F, Lan Y, Wang Y, Wang J, Yang G, Meng F, Han H, Meng A, Wang Y, Yang X. Endothelial Smad4 maintains cerebrovascular integrity by activating N-cadherin through cooperation with Notch. Dev. Cell. 2011; 20:291–302. [PubMed: 21397841]

Lobov IB, Renard RA, Papadopoulos N, Gale NW, Thurston G, Yancopoulos GD, Wiegand SJ. Delta-like ligand 4 (Dll4) is induced by VEGF as a negative regulator of angiogenic sprouting. Proc. Natl. Acad. Sci. USA. 2007; 104:3219–3224. [PubMed: 17296940]

Lu X, Le Noble F, Yuan L, Jiang Q, De Lafarge B, Sugiyama D, Bréant C, Claes F, De Smet F, Thomas JL, et al. The netrin receptor UNC5B mediates guidance events controlling morphogenesis of the vascular system. Nature. 2004; 432:179–186. [PubMed: 15510105]

Mahmoud M, Allinson KR, Zhai Z, Oakenfull R, Ghandi P, Adams RH, Fruttiger M, Arthur HM. Pathogenesis of arteriovenous malformations in the absence of endoglin. Circ. Res. 2010; 106:1425–1433. [PubMed: 20224041]

Miniati D, Jelin EB, Ng J, Wu J, Carlson TR, Wu X, Looney MR, Wang RA. Constitutively active endothelial Notch4 causes lung arteriovenous shunts in mice. Am. J. Physiol. Lung Cell. Mol. Physiol. 2010; 298:L169–L177. [PubMed: 19933399]

Mitchell D, Pobre EG, Mulivor AW, Grinberg AV, Castonguay R, Monnell TE, Solban N, Ucran JA, Pearsall RS, Underwood KW, et al. ALK1-Fc inhibits multiple mediators of angiogenesis and suppresses tumor growth. Mol. Cancer Ther. 2010; 9:379–388. [PubMed: 20124460]

Morikawa M, Koinuma D, Tsutsumi S, Vasilaki E, Kanki Y, Heldin CH, Aburatani H, Miyazono K. ChIP-seq reveals cell type-specific binding patterns of BMP-specific Smads and a novel binding motif. Nucleic Acids Res. 2011; 39:8712–8727. [PubMed: 21764776]

Murphy PA, Lu G, Shiah S, Bollen AW, Wang RA. Endothelial Notch signaling is upregulated in human brain arteriovenous malformations and a mouse model of the disease. Lab. Invest. 2009; 89:971–982. [PubMed: 19546852]

Murphy PA, Kim TN, Lu G, Bollen AW, Schaffer CB, Wang RA. Notch4 normalization reduces blood vessel size in arteriovenous malformations. Sci. Transl. Med. 2012; 4:ra8.

Niessen K, Zhang G, Ridgway JB, Chen H, Yan M. ALK1 signaling regulates early postnatal lymphatic vessel development. Blood. 2010; 115:1654–1661. [PubMed: 19903896]

Orlova VV, Liu Z, Goumans MJ, ten Dijke P. Controlling angiogenesis by two unique TGF-β type I receptor signaling pathways. Histol. Histopathol. 2011; 26:1219–1230. [PubMed: 21751154]

Park SO, Lee YJ, Seki T, Hong KH, Fliess N, Jiang Z, Park A, Wu X, Kaartinen V, Roman BL, Oh SP. ALK5- and TGFBR2-independent role of ALK1 in the pathogenesis of hereditary hemorrhagic telangiectasia type 2. Blood. 2008; 111:633–642. [PubMed: 17911384]

Park SO, Wankhede M, Lee YJ, Choi EJ, Fliess N, Choe SW, Oh SH, Walter G, Raizada MK, Sorg BS, Oh SP. Real-time imaging of de novo arteriovenous malformation in a mouse model of hereditary hemorrhagic telangiectasia. J. Clin. Invest. 2009; 119:3487–3496. [PubMed: 19805914]

Potente M, Gerhardt H, Carmeliet P. Basic and therapeutic aspects of angiogenesis. Cell. 2011; 146:873–887. [PubMed: 21925313]

Roman BL, Pham VN, Lawson ND, Kulik M, Childs S, Lekven AC, Garrity DM, Moon RT, Fishman MC, Lechleider RJ, Weinstein BM. Disruption of acvrl1 increases endothelial cell number in zebrafish cranial vessels. Development. 2002; 129:3009–3019. [PubMed: 12050147]

Scharpfenecker M, van Dinther M, Liu Z, van Bezooijen RL, Zhao Q, Pukac L, Löwik CW, ten Dijke P. BMP-9 signals via ALK1 and inhibits bFGF-induced endothelial cell proliferation and VEGF-stimulated angiogenesis. J. Cell Sci. 2007; 120:964–972. [PubMed: 17311849]

Seemann P, Brehm A, König J, Reissner C, Stricker S, Kuss P, Haupt J, Renninger S, Nickel J, Sebald W, et al. Mutations in GDF5 reveal a key residue mediating BMP inhibition by NOGGIN. PLoS Genet. 2009; 5:e1000747. [PubMed: 19956691]

Seki T, Yun J, Oh SP. Arterial endothelium-specific activin receptor-like kinase 1 expression suggests its role in arterialization and vascular remodeling. Circ. Res. 2003; 93:682–689. [PubMed: 12970115]

Shovlin CL. Molecular defects in rare bleeding disorders: hereditary haemorrhagic telangiectasia. Thromb. Haemost. 1997; 78:145–150. [PubMed: 9198145]

Shovlin CL. Hereditary haemorrhagic telangiectasia: pathophysiology, diagnosis and treatment. Blood Rev. 2010; 24:203–219. [PubMed: 20870325]

Stenzel D, Franco CA, Estrach S, Mettouchi A, Sauvaget D, Rosewell I, Schertel A, Armer H, Domogatskaya A, Rodin S, et al. Endothelial basement membrane limits tip cell formation by inducing Dll4/Notch signalling in vivo. EMBO Rep. 2011; 12:1135–1143. [PubMed: 21979816]

Suchting S, Freitas C, le Noble F, Benedito R, Bréant C, Duarte A, Eichmann A. The Notch ligand Delta-like 4 negatively regulates endothelial tip cell formation and vessel branching. Proc. Natl. Acad. Sci. USA. 2007; 104:3225–3230. [PubMed: 17296941]

Suzuki Y, Ohga N, Morishita Y, Hida K, Miyazono K, Watabe T. BMP-9 induces proliferation of multiple types of endothelial cells in vitro and in vivo. J. Cell Sci. 2010; 123:1684–1692. [PubMed: 20406889]

Tammela T, Zarkada G, Wallgard E, Murtomäki A, Suchting S, Wirzenius M, Waltari M, Hellström M, Schomber T, Peltonen R, et al. Blocking VEGFR-3 suppresses angiogenic sprouting and vascular network formation. Nature. 2008; 454:656–660. [PubMed: 18594512]

Taylor KL, Henderson AM, Hughes CC. Notch activation during endothelial cell network formation in vitro targets the basic HLH transcription factor HESR-1 and downregulates VEGFR-2/KDR expression. Microvasc. Res. 2002; 64:372–383. [PubMed: 12453432]

Testori J, Schweighofer B, Helfrich I, Sturtzel C, Lipnik K, Gesierich S, Nasarre P, Hofer-Warbinek R, Bilban M, Augustin HG, Hofer E. The VEGF-regulated transcription factor HLX controls the expression of guidance cues and negatively regulates sprouting of endothelial cells. Blood. 2011; 117:2735–2744. [PubMed: 21224470]

Urness LD, Sorensen LK, Li DY. Arteriovenous malformations in mice lacking activin receptor-like kinase-1. Nat. Genet. 2000; 26:328–331. [PubMed: 11062473]

Valdimarsdottir G, Goumans MJ, Rosendahl A, Brugman M, Itoh S, Lebrin F, Sideras P, ten Dijke P. Stimulation of Id1 expression by bone morphogenetic protein is sufficient and necessary for bone morphogenetic protein-induced activation of endothelial cells. Circulation. 2002; 106:2263–2270. [PubMed: 12390958]

Wacker A, Gerhardt H. Endothelial development taking shape. Curr. Opin. Cell Biol. 2011; 23:676–685. [PubMed: 22051380]

Zhong TP, Rosenberg M, Mohideen MA, Weinstein B, Fishman MC. gridlock, an HLH gene required for assembly of the aorta in zebrafish. Science. 2000; 287:1820–1824. [PubMed: 10710309]

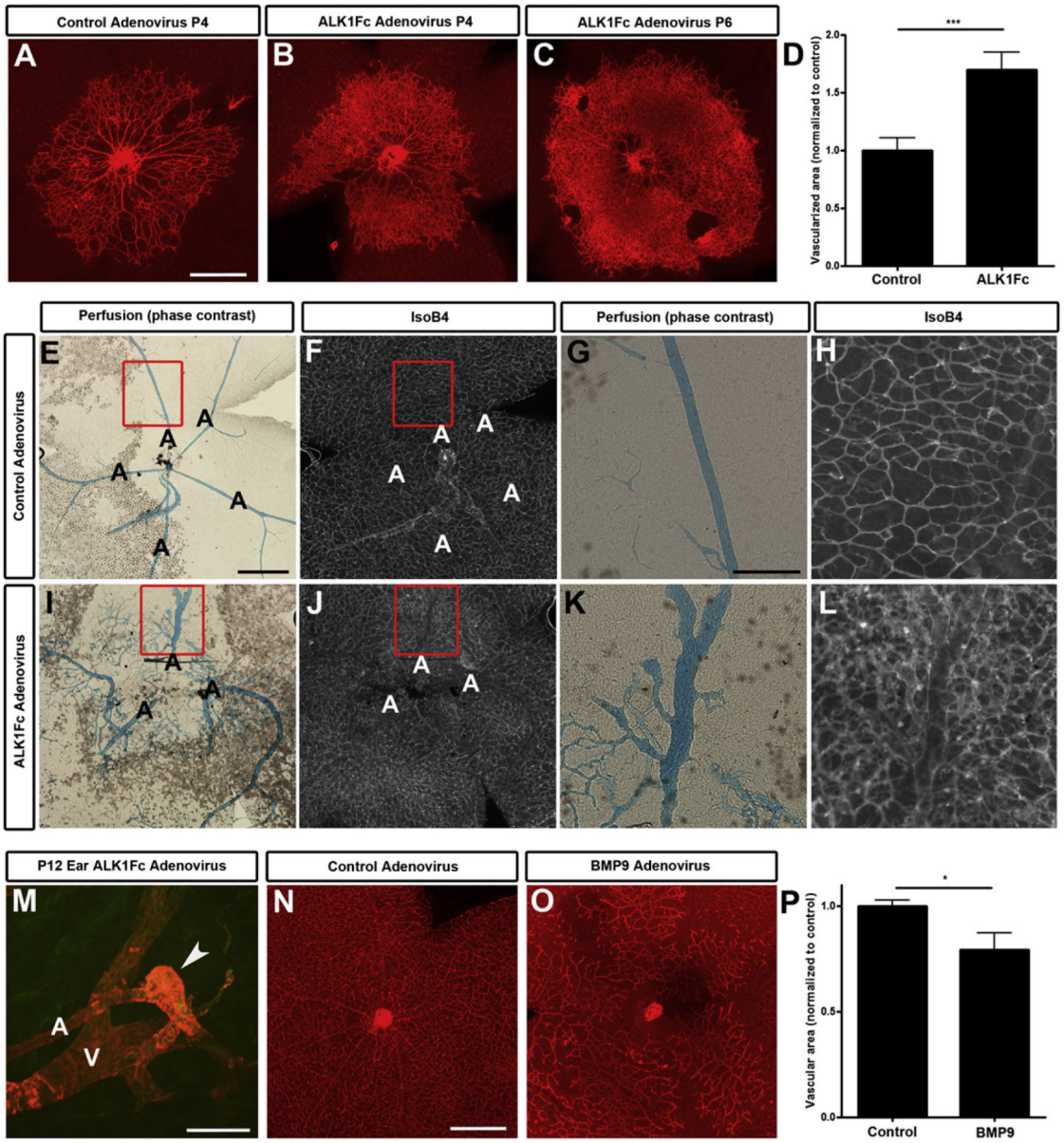

Figure 1. Alk1 Signaling Regulates Blood Vessel Morphogenesis

(A–C) IsolectinB4 staining of wild-type P4 (A and B) and P6 (C) retinal vessels after treatment with control (A) or ALK1Fc adenovirus (B and C). Scale bar, 500 μm. (D) Quantification of vessel density in the area of retina covered by vessels in control adenovirus compared with ALK1Fc adenovirus at P6 (n = 7 mice/group). (E–L) P12 arterial vascular patterns shown by blue latex dye injected into the left ventricle of control (E–H) and ALK1Fc (I–L) adenovirus-injected pups. (F), (H), (J), and (L) show the corresponding IsolectinB4 staining of retinal vessels. (G), (H), (K), and (L) are higher magnification pictures of boxes shown in (E), (F), (I), and (J). Note abnormal artery formation and hypervascularization in ALK1Fc-treated retinas (I–L). A, artery. Scale bars, 200 μm (E, F, I, and J) and 70 μm (G, H, K, and L). (M) SMA (red) and PECAM-1 (green) staining of P12

ear skin from ALK1Fc adenovirus-treated mice. Note the presence of an AV shunt (arrowhead). Scale bar, 100 μm.

(N and O) IsolectinB4 staining of wild-type P12 retinal vessels after treatment with control (N) or Bmp9 (O) adenovirus. Scale bar, 250 μm.

(P) Quantification of vessel density in control adenovirus compared with Bmp9 adenovirus at P12 (n = 5 mice/group).

All values are mean ± SEM. *$p < 0.05$; ***$p < 0.005$; Student's t test.

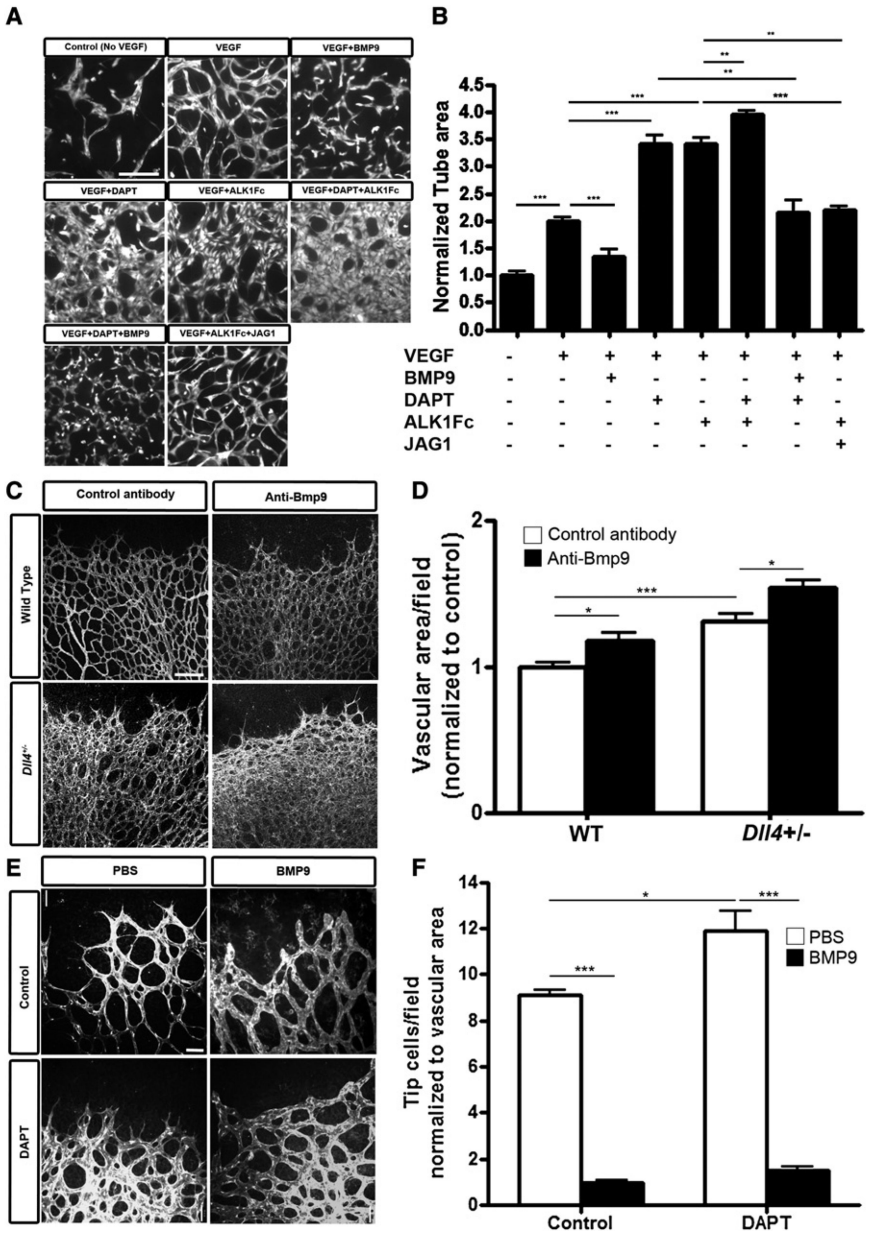

Figure 2. Effect of Notch and ALK1 Signaling on Endothelial Sprouting In Vitro and In Vivo

(A) Representative images of HUVECs sprouting in a fibrin gel in the presence or absence of ALK1 or Notch agonists and antagonists. Scale bar, 75 μm. (B) Quantification of tube surface area. Graphs represent the average of three to five experiments. (C) Representative images and vascular area quantification of P5 retinas from wild-type or *Dll4*$^{+/—}$ pups that received intraperitoneal injections of control or Bmp9 blocking antibody. Scale bar, 120 μm. (D) Quantification of vascular area at P5 (WT plus control antibody, n = 9 retinas; WT plus anti-Bmp9 antibody, n = 4 retinas; *Dll4*$^{+/—}$ plus control antibody, n = 9 retinas; *Dll4*$^{+/—}$ plus anti-Bmp9 antibody, n = 9 retinas).

(E) Representative images and quantification of tip cells of P5 retinas from pups injected with vehicle control or DAPT that received intraocular injections of PBS or BMP9. Scale bar, 36 μm.

(F) Quantification tip cells at the vascular front 16 hr after intraocular injection (n = 4 retinas for control PBS and BMP9; n = 6 retinas for DAPTPBS and BMP9).

All values are mean ± SEM. *p < 0.05; **p < 0.01; ***p < 0.005; Student's t test.

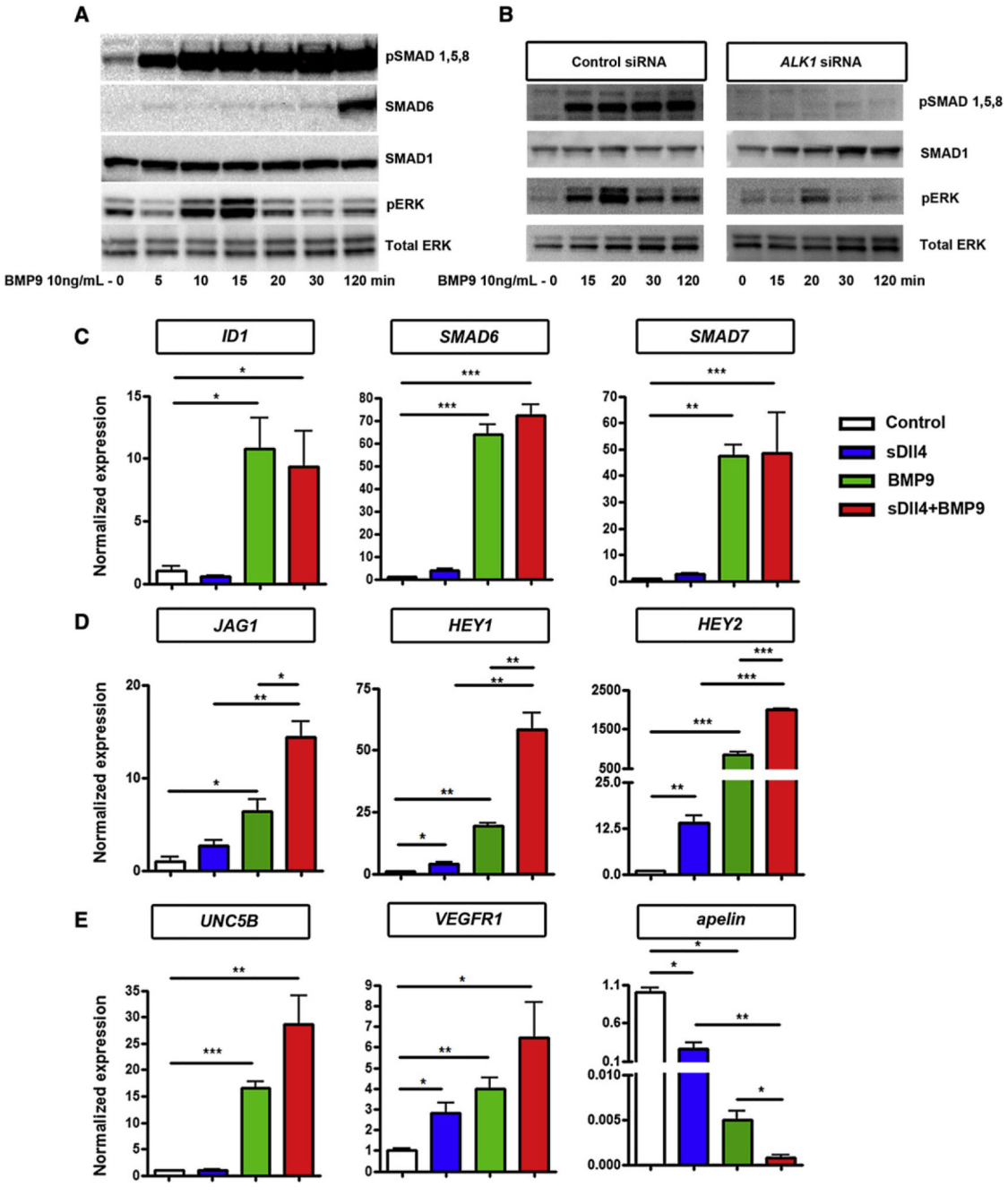

Figure 3. BMP9 Signals through ALK1 and Regulates Endothelial Gene Expression

(A and B) Western blot analysis of parental HUVECs (A) or control or *ALK1* siRNA-transfected HUVECs (B) following stimulation with 10 ng/ml BMP9 for up to 2 hr. (C–E) qPCR analysis of genes involved in SMAD signaling (C), Notch signaling (D), or tip cell specification (E) induced by ALK1 (BMP9) or Notch (sDll4) signaling in HUVECs, alone or in combination after 24 hr stimulation. Graphs represent the average of three to five experiments. All values are mean ± SEM. *$p < 0.05$; **$p < 0.01$; ***$p < 0.005$; Student's t test.

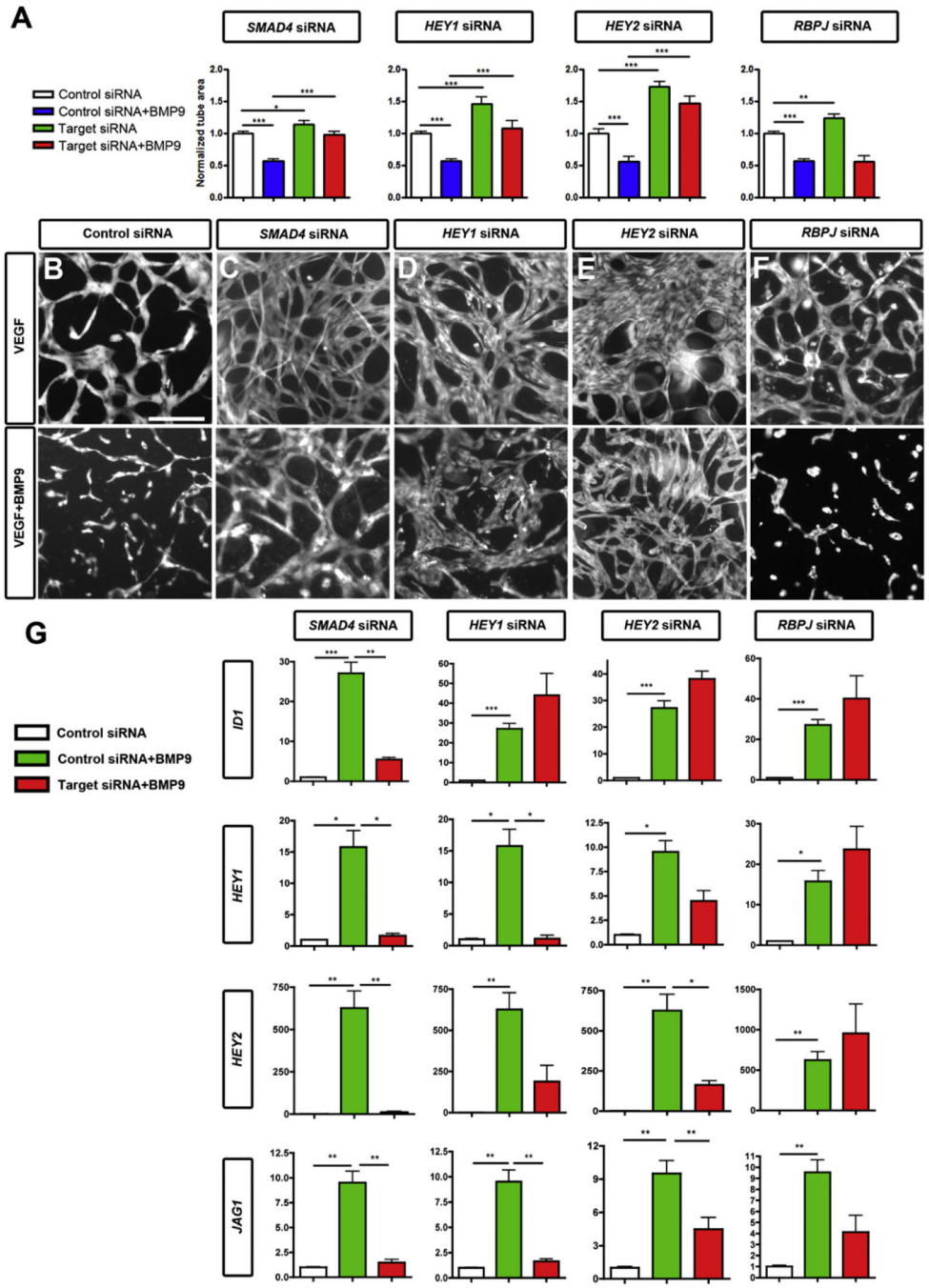

Figure 4. ALK1 Regulates Endothelial Sprouting and Gene Expression through SMAD Signaling and HEY

(A–F) Tube formation of siRNA-transfected HUVECs. (A) Quantification of tube surface area after 3 days of sprouting and 2 days of treatment with or without BMP9 10 ng/ml. (B–F) Representative images of endothelial tubes following siRNA transfection in the absence (top row) or presence (bottom row) of 10 ng/ml BMP9. Scale bar, 75 μm.

(G) qPCR analysis of genes induced by ALK1 after transfection with control, *SMAD4*, *HEY1*, *HEY2*, or *RBPJ* siRNA, with or without BMP9 stimulation. Graphs represent the average of three to five experiments.

All values are mean ± SEM. *p < 0.05; **p < 0.01; ***p < 0.005; Student's t test.

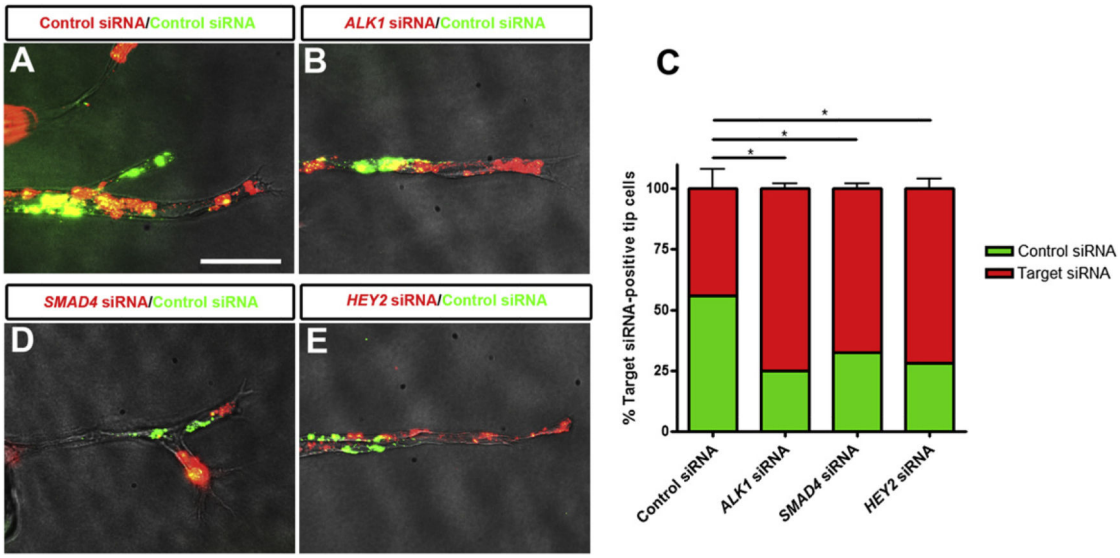

Figure 5. ALK1 Signaling through SMAD and HEY Prevents Tip Cell Specification

HUVECs transfected with siRNA were labeled with green or red fluorescent dyes, mixed, coated on microcarrier beads, and embedded in fibrin. (A, B, D, and E) Representative images of sprouts 4 days after siRNA transfection. Scale bar, 65 μm.

(C) Quantification of percentage of target siRNA-transfected cells at the tip position of sprouts. Sprouts on 25–30 beads were quantified per experiment. Graphs represent the average of three to four experiments. All values are mean ± SEM. *$p < 0.05$; Student's t test.

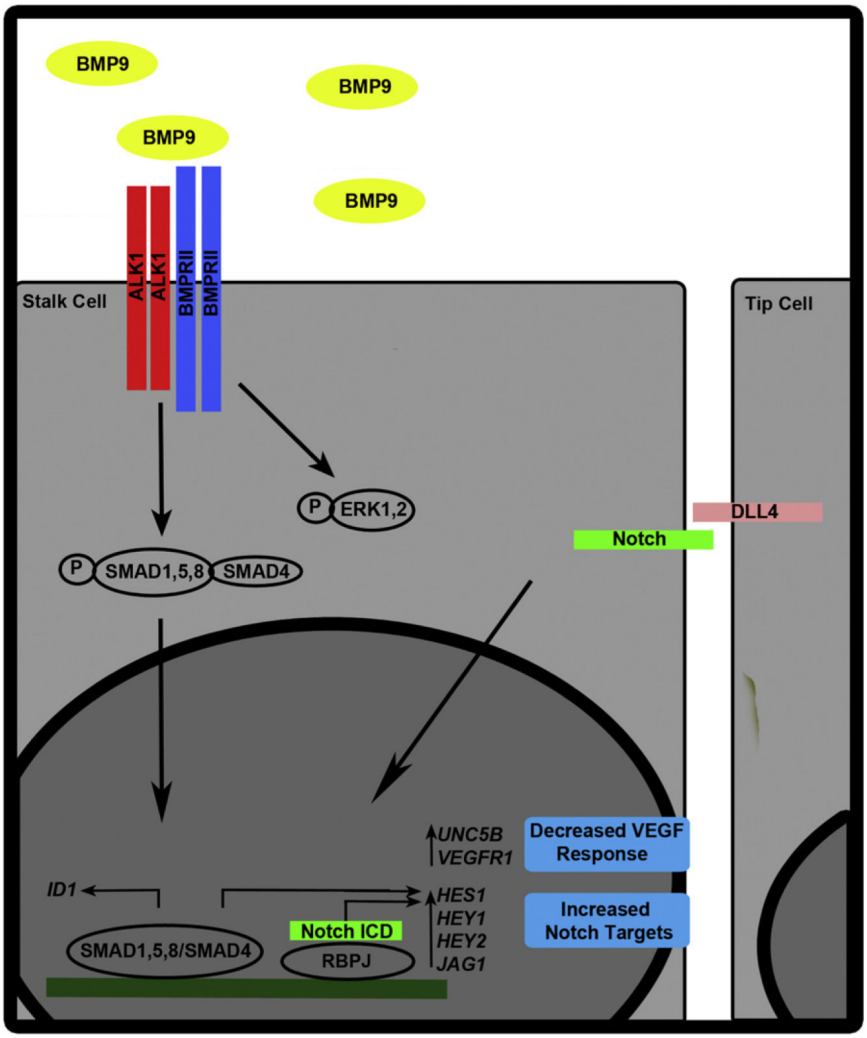

Figure 6. Working Model for ALK1 Signaling in ECs

The data suggest that ALK1 signaling, triggered upon BMP9 binding, activates SMAD1,5,8 signaling, which induces expression of *HES1*, *HEY1*, and *HEY2* together with Notch signaling. ALK1 also induces expression of UNC5B and VEGFR1, therefore reducing VEGF response and tip cell specification. This modulation of gene expression by Alk1 contributes to the stability and quiescence of the endothelium.